Author for correspondence:
David L. Hu
e-mail: hu@me.gatech.edu

Royal Society Publishing
Informing the science of the future

Snakes mimic earthworms: propulsion using rectilinear travelling waves

Hamidreza Marvi[1], Jacob Bridges[1] and David L. Hu[1,2]

[1]School of Mechanical Engineering, and [2]School of Biology, Georgia Institute of Technology, 771 Ferst Drive, Atlanta, GA 30332, USA

In rectilinear locomotion, snakes propel themselves using unidirectional travelling waves of muscular contraction, in a style similar to earthworms. In this combined experimental and theoretical study, we film rectilinear locomotion of three species of snakes, including red-tailed boa constrictors, Dumeril's boas and Gaboon vipers. The kinematics of a snake's extension–contraction travelling wave are characterized by wave frequency, amplitude and speed. We find wave frequency increases with increasing body size, an opposite trend than that for legged animals. We predict body speed with 73–97% accuracy using a mathematical model of a one-dimensional n-linked crawler that uses friction as the dominant propulsive force. We apply our model to show snakes have optimal wave frequencies: higher values increase Froude number causing the snake to slip; smaller values decrease thrust and so body speed. Other choices of kinematic variables, such as wave amplitude, are suboptimal and appear to be limited by ana-tomical constraints. Our model also shows that local body lifting increases a snake's speed by 31 per cent, demonstrating that rectilinear locomotion benefits from vertical motion similar to walking.

1. Introduction

Snakes have long flexible bodies that enable them to easily traverse complex ter-rain, such as sand, foliage, narrow crevices or tree trunks. In narrowly confined terrain, snakes use a gait called 'rectilinear locomotion' to propel themselves in a straight line, similar to earthworms. Understanding how snakes propel themselves unidirectionally provides a more complete picture of why snakes are so versatile in environments where both legs and wheels are known to fail. In terms of practical applications, rectilinear locomotion may provide added versatility to limbless snake-like robots, designed for use in search-and-rescue processes during natural disasters [1,2]. Rectilinear locomotion may also be implemented in the control of medical snake-robots used to reach parts of the human body that physicians have difficulty accessing [3]. Such applications involve locomotion through tight crevices and so require the application of rectilinear locomotion.

Rectilinear locomotion is one of four 'gaits', or modes of snake locomotion, each specialized for a particular type of terrain. Slithering is applied on flat surfaces or through structured environments such as between rocks, used as push points [4]. Sidewinding is used on granular surfaces such as sand [5]. An accordion-like concertina motion is used within intermediate-sized crevices that are much wider than the snake's diameter [6]. Within more tightly confined crevices, snakes cannot use these gaits because of the lack of space and so instead use rectilinear locomotion. For example, rectilinear locomotion is used to travel vertically upward along the interstices of tree bark, across narrow tree boughs, and alongside walls. We have observed snakes using rectilinear locomotion to crawl out of their own skin during shedding, a periodic event that removes parasites and permits growth. The body trajectory for rectilinear locomotion is linear, which minimizes the path length travelled by parts of the body and, in turn, the sounds produced. Thus, rectilinear locomotion is naturally applied to stealthy activities such as stalking prey.

Rectilinear locomotion is the least studied of the snake gaits. Home [7] pub-lished the first study of rectilinear locomotion nearly two centuries ago,

Figure 1. Snake species used in our experiments. (*a,b*) Boa constrictor, (*c*) Dumeril's boa and (*d*) Gaboon viper. Snakes (*b*)–(*d*) perform rectilinear motion against a wall. (Online version in colour.)

describing rectilinear locomotion as 'rib-walking'. He observes that the ribs of *Coluber constrictor* move forward in sequence, similar to the feet of a caterpillar. Since then, several studies have overturned the rib-walking hypothesis [8–10]. The most extensive experimental study on rectilinear locomotion is conducted by Lissman [10], who studies two specimens of *Boa occidentalis*. He uses X-ray imaging to show a snake's ribs maintain their fixed spacing during propulsion. He reports ventral kinematics, proposing propulsion is achieved using travelling waves of muscular contraction and expansion on the ventral surface. This finding draws attention because it shows the snake's skeletal structure performs no lever action, a rare occurrence among locomotion of vertebrates. In rectilinear locomotion, a snake is propelled by virtue of its soft body alone, as an earthworm [10].

The energetic expenditure of rectilinear motion is unknown, but promises to be low given the low inertia and lateral movement involved. The traditional measure of the rate of working is the net cost of transport (NCT) of snakes, found by measuring the oxygen consumption of snakes on treadmills. The most efficient gait is sidewinding (NCT = 8 J kg^{-1} m^{-1}), followed by slithering (23 J kg^{-1} m^{-1}) and lastly concertina motion (170 J kg^{-1} m^{-1}) [5,11]. The NCT of rectilinear locomotion has yet to be measured. To improve this situation, we perform a calculation of the physical rate of work in rectilinear motion in §5.4.

Unidirectional limbless locomotion has also drawn the attention of theoreticians. One of the simplest models proposed is the two-anchor model, consisting of a two-segment extensible worm that uses frictional anisotropy to propel itself [12]. Keller & Falkovitz [13] present a continuous model for a series of these segments connected together. They find trends for period and average speed as a function of body mass that are qualitatively similar to Gray's [14] observations of worms. Moreover, they derive the relationship between the time-rate of change of the worm's internal pressure and body speed. Zimmermann *et al.* [15] also present a discrete model for worm locomotion considering nonlinear asymmetric friction.

In this combined experimental and theoretical study, we report on the rectilinear locomotion of three species of snakes on a horizontal substrate. In §2, we describe our methods. We proceed in §3 with our theoretical model for rectilinear locomotion. In §§4 and 5, we present our experimental results and our numerical predictions. We discuss the unique wave frequency scaling in §6. Lastly, in §7, we summarize the implications of our work and suggest directions for future research.

2. Methods

2.1. Animal care

To identify snakes that reliably perform rectilinear locomotion, we initially observe 21 species of snakes, listed in the electronic supplementary material, S1. Among these species, the vast majority do not perform rectilinear locomotion reliably on our Styrofoam trackway. We here report upon three species that perform well. Among them, we filmed six individuals, including three juvenile red-tailed boa constrictors (*Boa constrictors*, figure 1*a,b*), two Dumeril's boa constrictors (*Boa dumerili*, figure 1*c*) and one Gaboon viper (*Bitis gabonica*, figure 1*d*).

Red-tailed boas are purchased from Florida Herps. They are fed weekly and housed in separate terrariums with controlled temperature and humidity conditions at Georgia Tech. Dumeril's boas and the Gaboon viper are housed at Zoo Atlanta, also in separate cages with controlled conditions. All animal care and experimental procedures are approved by IACUC.

The lengths and masses of the snakes studied are given in table 1. As reported in table 1, snake mass scales linearly with body length (m(kg) = 0.027L(cm), r^2 = 0.73). Hereon, we report allometric results in terms of body length.

2.2. Friction measurements

We line the bottom of our trackway with open-cell rigid Styrofoam. In our previous work [6], this surface was effective at engaging a snake's ventral scales with surface asperities. We

Table 1. Animal subjects. The number of snakes (N) used in our experiments, their lengths (L), masses (m), forward and backward sliding friction coefficients (μ_f and μ_b), and number of naturally occurring spots (n). The data for each individual snake are provided in the electronic supplementary material, S11.

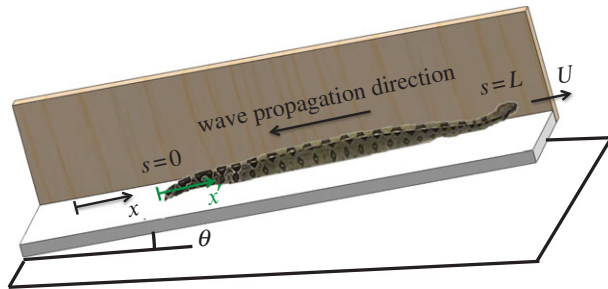| species	N	L (cm)	m (kg)	μ_f	μ_b	n
Boa constrictor	3	53.3 ± 1.5	0.06 ± 0.01	0.3 ± 0.06	0.42 ± 0.05	23 ± 2
Dumeril's boa	2	175.5 ± 10.6	5.7 ± 1.1	0.017 ± 0.002	0.06 ± 0.01	25 ± 1
Gaboon viper	1	120	2.26	0.12	0.32	20

Figure 2. Schematic of the apparatus used to study rectilinear locomotion. Here, θ is the inclination angle with respect to the horizontal. The front wall (not shown) is composed of Plexiglas. The ground coordinate frame (x) and moving coordinate frame (x') are indicated by the arrows. The direction of wave propagation in rectilinear locomotion is opposite to the direction of motion. (Online version in colour.)

measure friction coefficients of conscious snakes using the inclined-plane method, developed in our previous work [4,6].

2.3. Trackway construction, filming and image processing

We construct a 5 m × 60 cm rectangular trackway to provide a controlled environment for studying rectilinear locomotion. A single wooden sidewall guides the snake along the trackway, as shown in figure 2. However, this sidewall does not provide the snake with any significant thrust force as discussed in the electronic supplementary material, S2. The trackway's substrate consists of a series of five blocks of Styrofoam. Underneath the Styrofoam, reinforcement is provided using two wooden planks of thickness 5 cm to reduce bending owing to the combined animal and trackway weight. The trackway length measures 10 snake body lengths for the boa constrictor, three body lengths for the Dumeril's boas and four body lengths for the Gaboon viper. This length ensured a large number of periods are obtained from each trial.

Experiments are conducted outdoors. We film snakes from the side using a high-definition digital video camera (Sony HDRXR200). Open source tracker, a video analysis modelling tool (www.cabrillo.edu/dbrown/tracker/), is used to measure the time course of the positions of approximately 20 naturally occurring spots on the snake. Average body speeds are measured over 7–15 periods. The wave processing algorithms and peak detection method are discussed in the electronic supplementary materials, S3 and S4.

2.4. Definition of reference frames

To describe body kinematics, we begin with a formal definition of two reference frames illustrated in figure 2. Most previous work on snakes uses two- or three-dimensional coordinate frames. However, for rectilinear locomotion, we require kinematics and dynamics along a single dimension. Kinematics are described by unidirectional contractions and extensions.

Body lifting is prescribed using a direction-dependent friction coefficient in §4.1.

Two reference frames are of interest: the first is the ground coordinate system x which is fixed to the trackway. The second is a moving coordinate frame x' fixed to the snake's tail, and travels with the snake's steady body speed V. Electronic supplementary material, videos S5 and S6 show snakes' rectilinear motion in these two coordinate systems. Initially, the origins of both coordinate frames coincide at the tip of snake's tail. For each time t, the relation between the two coordinate frames is

$$x' = x - Vt, \tag{2.1}$$

where distances are given in centimetres and time in seconds. The use of the snake coordinate frame (x') permits prescription of kinematics without reference to centre of mass. In this frame, positions of points on the body are purely oscillatory owing to the passage of a travelling wave, as shown in the electronic supplementary material, video S6. The snake spans a distance from its tail ($s = 0$) to its head ($s = L$), where L is the snake length. We characterize travelling wave kinematics using time t and distance s along the snake, measured from the tail. Travelling waves propagate towards the tail, in the negative x'-direction.

3. Model

We model snakes as one-dimensional, n-linked crawlers (figure 3). For this purpose, we adopt a model we developed previously for concertina locomotion [6]. Snakes are discretized into n nodes connected in series by $n - 1$ inter-nodal elements, or extensible 'muscles', whose length dynamics characterize the travelling wave. The inputs to our model are the snake's travelling wave kinematics and friction coefficients, both measured in our experiments. The output to the model is the snake's centre of mass position $\bar{x}$. For each node in contact with the substrate, we use a sliding friction law in which the friction force is

$$F_i = -\mu_i F_N \text{sgn}(\dot{x}_i), \tag{3.1}$$

where F_N is the normal force owing to the node's weight, and $\dot{x}_i$ is the node's speed. The sliding friction coefficients μ_i of the ventral surface are μ_f and μ_b, respectively, for the forward and backward directions. We apply Newton's second law to each of the n nodes, considering both friction and inter-nodal forces. Details are given in Marvi & Hu [6]. The non-dimensionalized governing equation for the centre of mass is

$$Fr\ddot{\bar{x}} = \frac{\cos\theta}{n}\left[-\mu_f\sum_{i=1}^{n}H(\dot{x}_i) + \mu_b\sum_{i=1}^{n}H(-\dot{x}_i)\right] - \sin\theta, \tag{3.2}$$

where $H(x) = \frac{1}{2}(1 + \text{sgn}x)$ is the Heaviside step function, θ is the inclination angle, and Fr is the Froude number defined as

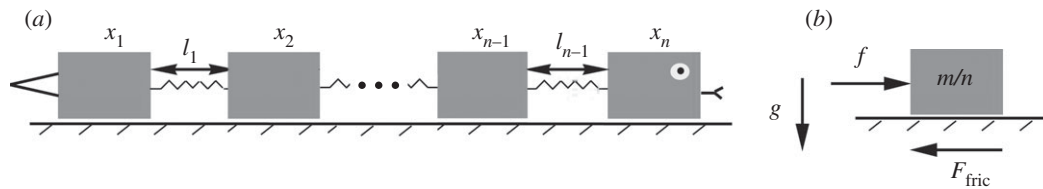$$Fr = \frac{\text{inertia}}{\text{gravity}} = \frac{L}{\tau^2 g}, \tag{3.3}$$

Figure 3. Mathematical model for rectilinear locomotion. (*a*) Schematic of *n*-link crawler and (*b*) forces applied to each block.
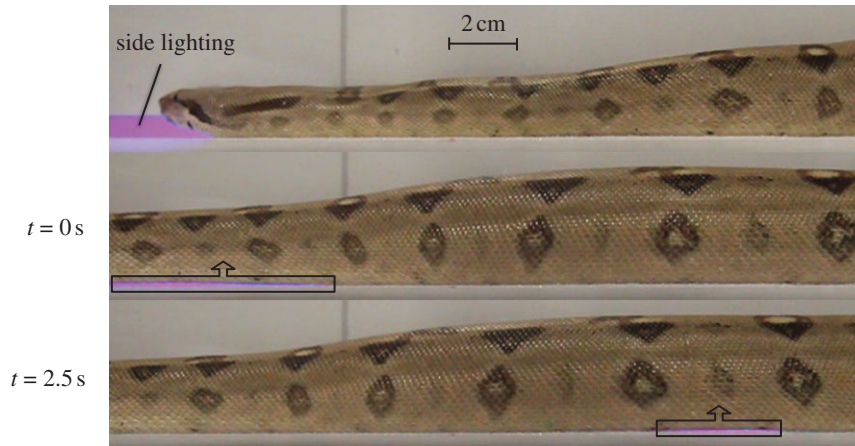

Figure 4. A boa constrictor lifting parts of its body during rectilinear locomotion. We shine a purple light from the side which passes underneath the snake to reveal lifted parts. For clarity, lifted regions are denoted by a black outline and an arrow indicating direction of lifting. The body is lifted approximately 1 mm and the corresponding wave speed is 6 cm s^{-1}. (Online version in colour.)

where L is body length, τ is the period of the extension–contraction and g is the gravitational acceleration. According to our experiments, the Froude number is very small ($Fr \leq 2 \times 10^{-4}$) indicating inertial force is extremely small compared with gravitational force. In comparison, Froude numbers for other snake gaits are one to two orders of magnitude larger: $Fr \approx 0.002$–0.016 for concertina motion [6] and $Fr \approx 0.02$ [4] for slithering. Clearly, rectilinear locomotion has lower inertial forces than the other snake gaits.

The low-Froude number for rectilinear locomotion is consistent with the high repeatability of our experiments. If a snake has negligible inertia, then snakes need very little lead time to reach steady speed. Moreover, each period of motion is dynamically similar to the first period starting from rest. We see evidence of these attributes in our experiments. Body speed is constant from beginning to end of the trial. Moreover, we observe a nearly instantaneous ramp up to steady speed at the beginning of the trackway. A similarly instantaneous deceleration is observed at the end of the trackway.

4. Experimental results

In this section, we present measurements of snake body lifting, frictional properties and kinematics, which together will be used in our model to predict snake speed. Kinematics are presented in terms of travelling waves along the ventral surface. We lastly present scaling of kinematics among the three snake species we used in this study.

4.1. Snakes lift ventral surfaces to move forward

Figure 4 shows a video sequence of a boa crawling forward by lifting its ventral surface (see the electronic supplementary material, video S7). We visualize this body lifting by shining

a purple light from one side of the snake. In the first frame, the majority of the body is pressed against the ground, which prevents the side lighting from reaching the camera. At $t = 0$ s, the front of the body is lifted. At $t = 2.5$ s, this wave progresses backwards 15 cm at a speed of 6 cm s^{-1}, and is marked by a newly lifted segment of the snake. The continuous motion of this lifted region is shown in the electronic supplementary material, video S7. We observe the wave of lifting propagates at the same speed as the wave of contraction, in correspondence with the assumptions of our model. We estimate lift height to be 1 mm by measuring the thickness of the light sheet visible beneath the ventral surface.

Why do snakes lift 1 mm in height? We can rationalize this length scale using a simple scaling argument. The primary reason for lifting is to save energy. Thus, we hypothesize the energy expended to lift must be less than the frictional dissipation of sliding forward without lifting. The energy spent on lifting is $m_l g \Delta h$, where m_l is the mass of the snake's lifted section, g is the gravitational acceleration and Δh is the lift height. If the snake did not lift, then it would dissipate a frictional energy $\mu_f m_l g \Delta x$, where μ_f is the forward friction coefficient, and Δx is body displacement in the direction of motion. For a boa constrictor with $\mu_f = 0.3$ and a forward displacement corresponding to the wave amplitude, $\Delta x = 0.27$ cm, we find Δh should be less than 0.8 mm to keep the lifting cost less than friction dissipation. This value is comparable to that measured, in confirmation of our hypothesis. Using similar methods, we predict the Gaboon viper must lift to a comparable height of 1.9 mm. We find the Dumeril's boa has the smallest required lift height, a value of only 0.3 mm, because it has the lowest friction coefficient of the three snakes studied. These estimates of ventral surface lifting will be incorporated into our prediction of snake energy expenditure in §5.4.
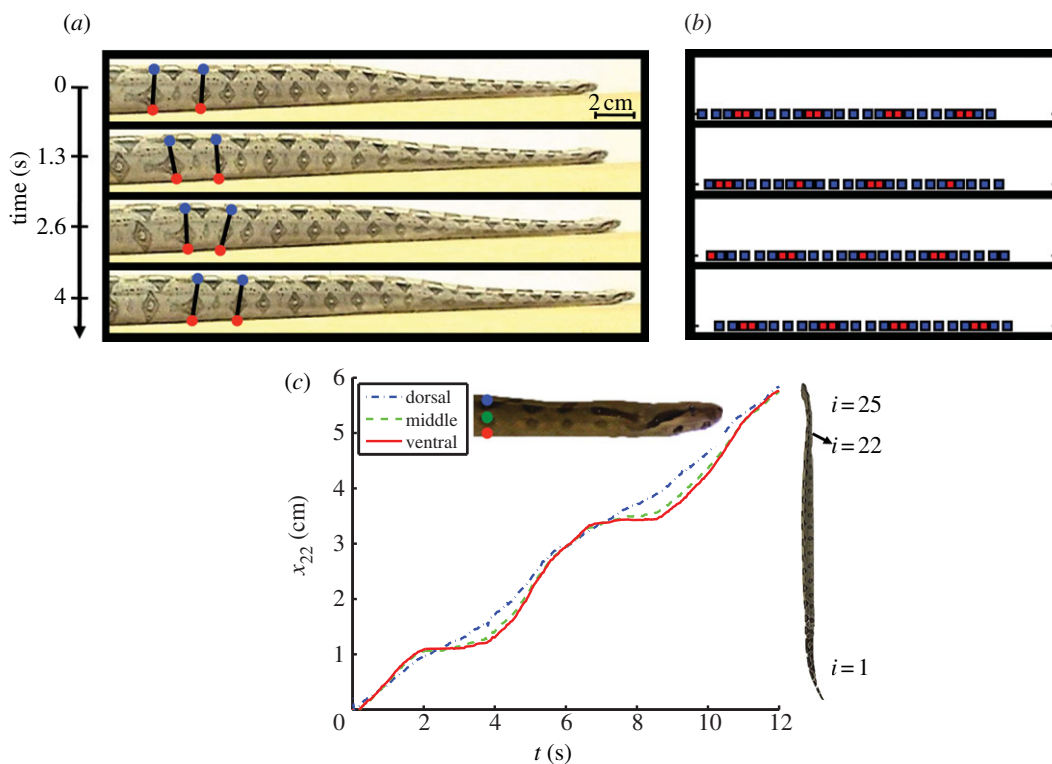
Figure 5. Unidirectional contraction–extension wave during rectilinear locomotion. (*a*) Image sequence of a boa constrictor performing rectilinear locomotion. The black lines follow the naturally occurring patterns on the snake skin and their spacing demonstrates the muscular strain at varying heights along the body. (*b*) One period of our *n*-link crawler model. The red blocks correspond to anchorage points. (*c*) Time course of the distance travelled by the 22nd spot on the snake, as shown in the inset. The solid, dashed, and dot-dashed lines indicate muscular travelling waves at three different elevations across the snake body: ventral, middle and dorsal. (Online version in colour.)

4.2. Friction coefficients

Table 1 shows the sliding friction coefficients of conscious snakes, measured on an inclined plane. The Gaboon viper ($\mu_b = 0.32$) and red-tailed boas ($\mu_b = 0.42 \pm 0.05$) have the highest friction coefficients, nearly five to seven times that of Dumeril's boas ($\mu_b = 0.06 \pm 0.01$). This difference is likely due to the difference in their habitat: Gaboon vipers and red-tailed boas live arboreally in rainforests and woodlands and so need high friction to climb trees. Dumeril's boas are terrestrial snakes, whose low friction coefficients make them poor climbers [16].

We observe in our experiments that snakes lift their bodies to move forward, an analogous behaviour to legged animals which lift the leading foot rather than drag it on the ground. This indicates the forward friction coefficients reported in table 1 are not dynamically relevant during locomotion. Thus, we prescribe the effective forward friction coefficient μ_f be zero in our modelling:

$$\mu_f = 0. \qquad (4.1)$$

4.3. Tracking of body markers

To characterize the travelling wave, we track the position of 20–26 naturally occurring body markers, whose spacings are roughly equal on a given snake. Electronic supplementary material, video S8 illustrates the tracked markers on a Dumeril's boa. As discussed in the electronic supplementary material, S9, we consider only the ventral surface anterior to the tail. Figure 5*a,c* shows the muscular travelling waves across the snake body. As shown in figure 5*c*, the ventral surface has the largest wave amplitude compared with middle and dorsal levels. Hereon, we report only on waves at the

ventral surface, which is in contact with the substrate. Each point on the snake undergoes a periodic motion (period $\tau = 2$–5 s). The combination of a long trackway (three to 10 body lengths) and slow speed of the snakes (1–6 cm s^{-1}) permits us ample data on the travelling wave. We discard the first and last period of motion along the trackway and analyse the remaining nine periods of motion for red-tailed boas, seven periods of motion for Dumeril's boas and 15 periods for the Gaboon viper.

Consider the locomotion of the red-tailed boa; analysis of other snakes proceeds similarly. Figure 6*a* shows the time course of position for $n = 25$ naturally occurring markers. The markers lie low on the snake's flanks but are visible just above the ground, as shown in figure 4. In figure 6*a,b*, we plot position in the ground reference frame x in order to show the distance travelled. The green curve on this plot corresponds to the position of the snake's head. Purple and red colours represent the snake's middle and tail, respectively.

The black arrows in figure 6*a* indicate the direction of the travelling wave; the magnitude of the slope of these arrows corresponds to the sum of magnitudes of the snake speed V and wave speed V_w. Figure 6*b* shows a magnified view of three points near the snake's head. These points perform a forward–backward oscillation combined with a constant speed in the forward direction.

The blue curve next to $i = 19$ in figure 6*a* shows the position of the 19th marker from the snake's tail. Figure 6*c* shows this position x' in the moving frame of the snake. We curve fit the position data x' to the travelling wave equation

$$x'(s, t) = A \sin(\omega t + ks) + s. \qquad (4.2)$$

To determine the parameters in equation (4.2), we use the curve-fitting algorithm discussed in the electronic
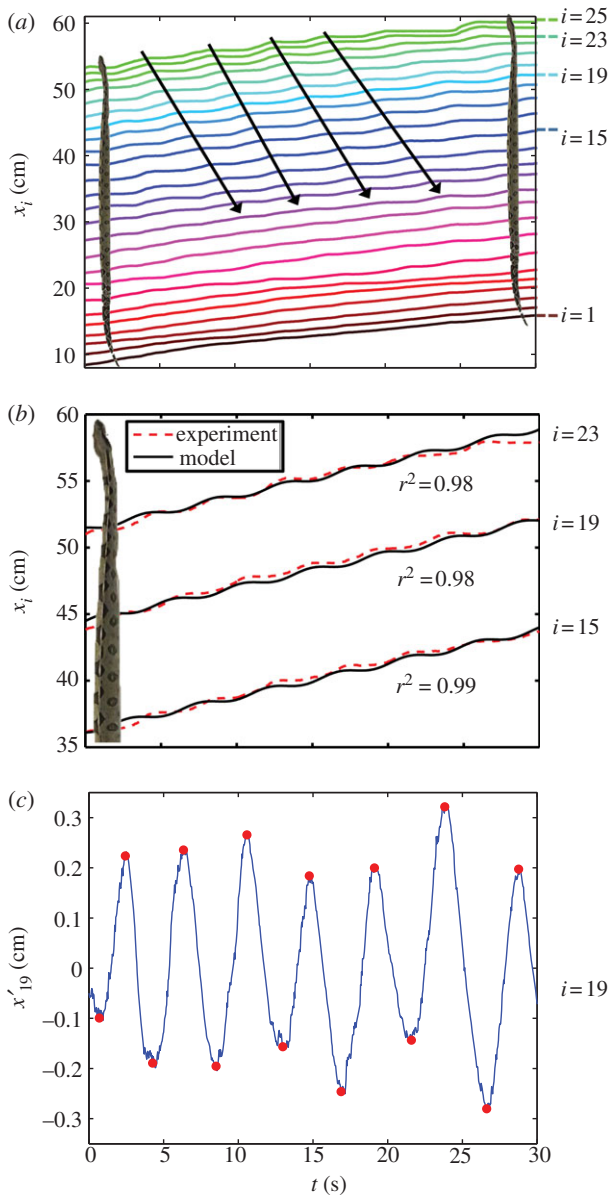
Figure 6. Body kinematics. (a) Time course of positions of 25 dots on the snake's body. The slope of the arrows has magnitude equal to absolute snake speed plus wave speed. (b) Time course of points 15, 19 and 23, as labelled in (a). (c) Peak detection of the travelling wave in the snake coordinate system. The noise in this plot has amplitude of around 0.2 mm, and is due to image processing noise. (Online version in colour.)

supplementary materials, S3 and S4. This algorithm is applied to each marker along the snake for seven to 15 periods, yielding values for the wave parameters. Figure 7 shows the relation between these wave parameters and the snake's body length. Averages and standard deviations are taken across all n body markers on a snake performing rectilinear locomotion for several periods (where n for each individual is given in table 1). We report means and standard deviations of different experimental parameters for each individual snake in figures 7 and 9. Wave parameters were quite uniform: standard deviations of less than 20 per cent were found for all, with the exception of a single red-tailed boa specimen which had a standard deviation of 40 per cent.

We used JMP software to determine statistical significance of measured wave parameters. The results of our statistical analysis are summarized in table 2. We determine the effect of body length L on several parameters, including snake mass m, speed V, wave speed V_w, wave amplitude A, wave

frequency f and wavelength λ. Body length has a statistically significant effect on all parameters, with a significance level of $\alpha = 0.01$, with the exception of wavelength λ.

4.4. Scaling of kinematics

Waveform parameters are found to depend upon body size, as shown in figure 7a–d. In previous studies, such trends are typically described using power laws. However, the small range in body length (factor of four) prevents us from properly extrapolating power laws. We instead report in table 2 the slopes of linear trend lines for wave speed, amplitude and frequency as a function of body length. As a consequence of these trends, body speed also increases linearly with body length as shown in figure 8 ($r^2 = 0.79$). Curve-fitting is quite accurate across these variables, despite our physical constraint that the lines have zero-intercept ($r^2 = 0.81 - 0.95$). We comment on the physical significance of these trends in turn.

Travelling waves have exceedingly small amplitude compared with body length: their ratio is $0.004 - 0.013$. Such small amplitudes are atypical compared with other snake gaits. For instance, the amplitude in concertina and slithering is $0.1 - 0.14$ body length [4,6]. As we will show in our modelling in §5.2, the low amplitude in rectilinear locomotion is the primary reason the gait is so slow.

Rectilinear locomotion is a slow mode of locomotion: speeds are only $0.2-6$ cm s^{-1}, or $0.02-0.07$ body lengths per second, for the $50-180$ cm snakes studied. It typically takes $14-50$ s to travel a single body length. The speeds of the boas in our study are comparable to those found by Lissman. He measured a speed of 0.37 cm s^{-1} on glass for two *B. occidentalis* (length 58.5 ± 2.2 cm) [10]. Other gaits performed by related species are much faster. For example, a 90 cm Rosy Boa (*Lichanura trivirgata*) can slither at 10 cm s^{-1} on horizontal ground partially covered with small plants [17]. Indeed, rectilinear locomotion is not used for its high speed.

Travelling waves are fast, ranging from 5 cm s^{-1} in the red-tailed boas to 25 cm s^{-1} in the Dumeril's boa. The high speed of the travelling wave is clearly visible in the electronic supplementary materials, videos S5–S8: waves tend to zip down the body while the snake lumbers forward slowly. Across the snakes studied, wave speed is three times body speed ($r^2 = 0.82$).

Wavelength indicates how many waves are visible at a given moment. The wavelength-to-body length ratio is 0.35 ± 0.14. Thus, at each instant, two to three waves are present along the body. This is consistent with previous reports by Lissman of two simultaneous travelling waves in *B. occidentalis* [10].

5. Numerical results

We now present predictions from our numerical model. We investigate the effect of changes in kinematics and friction coefficients on snake body speed. We report results only for the female Dumeril's boa, the fastest snake in our study, but these methods may be applied to other snakes in our study. The inputs to the model include snake friction coefficients, given in table 1 and equation (4.1) and travelling wave kinematics, given in figure 7. We change each of these inputs systematically in the following parameter study. We begin in §5.1 by using the model to predict the stationary points of the snake on the ground. We then proceed in §5.2 to predict how changes in one kinematic variable affect snake speed. In §5.3, we predict how body lifting would
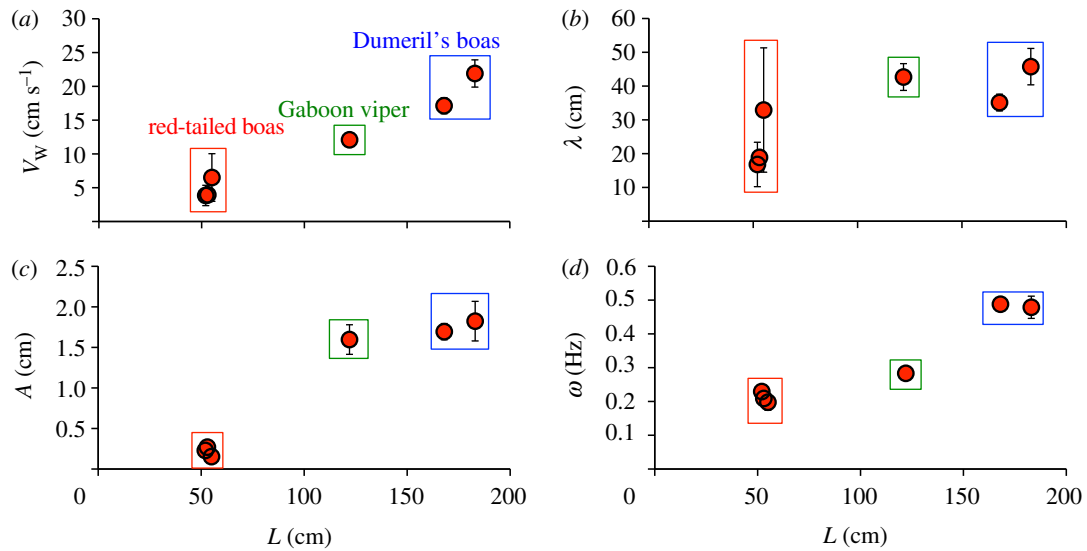
Figure 7. Scaling of wave kinematics. (a) Wave speed V_w, (b) wavelength λ, (c) wave amplitude A and (d) wave frequency ω of snakes in rectilinear locomotion. (Online version in colour.)

Table 2. The effect of snake body length L, on mass m, body speed V, wave speed V_w, wave amplitude A, wave frequency f, wavelength λ, percentage of body at rest and partial cost of transport PCT. Body length has a statistically significant effect, up to a significance level of $\alpha = 0.01$, on all parameters except λ, PCT, percentage of body at rest and PCT. F is the F-statistic and p is the p-value.

		L (cm)				
		slope	intercept	r^2	F	p
mass	m (kg)	0.0267	0	0.73	29.15	0.0029*
body speed	V (cm s^{-1})	0.0275	0	0.79	44.35	0.0012*
wave speed	V_w (cm s^{-1})	0.107	0	0.95	367.19	<0.0001*
wave amplitude	A (cm)	0.01	0	0.86	93.35	0.0002*
wave frequency	f (Hz)	0.0028	0	0.81	191.02	<0.0001*
wavelength	λ (cm)	0.158	15.4	0.64	6.99	0.0573
percentage of body at rest	% of body at rest	−0.0002	0.27	0.024	0.098	0.77
partial cost of transport	PCT (J kg^{-1} m^{-1})	0.003	1.32	0.005	0.018	0.9

improve body speed. Lastly, in §5.4 we discuss the energetic cost of rectilinear locomotion.

We use numerical simulation to integrate the model presented in §3. The inputs to the model are described in the electronic supplementary material, S10. The snake's prescribed travelling wave, equation (4.2), in conjunction with the governing differential equation (3.2) provide a system that we integrate over several periods to determine steady body speed. We use Matlab to find the numerical solution to this system. We apply the Dormand–Prince pair method, a member of the Runge–Kutta family of ordinary differential equation solvers, to find the solution of equation (3.2) numerically [18]. Using a dimensionless time step $\Delta t = 10^{-4}$, we solve equation (3.2) iteratively to determine the position of the snake's centre of mass $\bar{x}(t)$.

5.1. Model predictions of stationary points and body speed

Figure 5a,b and electronic supplementary material, video S8 compare one period of rectilinear locomotion of our n-linked crawler model to that of a snake. Red blocks correspond to stationary points on the snake's ventral surface, where we define stationary points as those with velocities less than 15 per cent of body speed. These stationary points are important to track because only these points generate thrust.

Figure 9 shows the relation between body length and percentage of the body that is instantaneously stationary, as found using our image analysis. We found 18–35% of the snake body is instantaneously stationary. The uniform distribution of such 'push points' along the body enables the snake to generate thrust even if the body is on heterogeneous slippery terrain. For example, if the middle of the snake is crossing a puddle, then both the front and back end can still generate thrust to push it across.

Figure 8 shows the relation between body length and speed. Experiments are given by the red symbols and the model prediction by the blue. The model predictions based on friction coefficient and body kinematics are highly accurate. Accuracy ranges from 97 per cent accuracy for the Dumeril's boa to 73 per cent accuracy for the red-tailed boa.
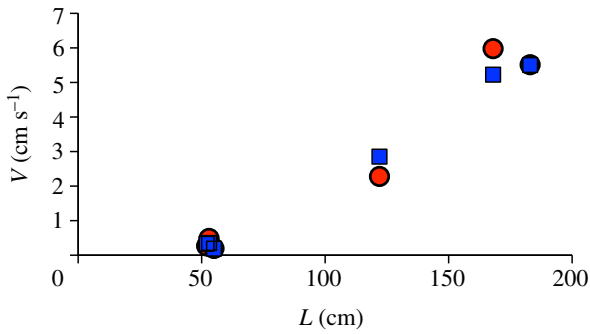
Figure 8. Snakes' body speed V compared with model predictions. Red circles denote experiment, blue squares denote model. (Online version in colour.)
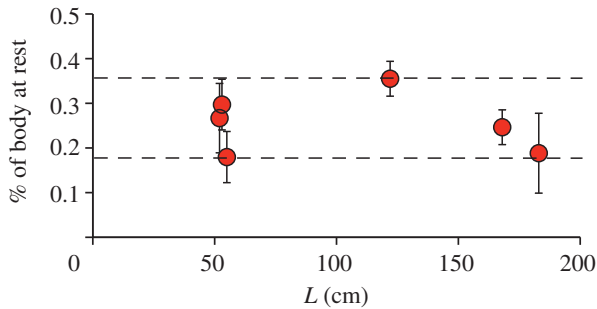

Figure 9. Fraction of the snake body that is instantaneously stationary. (Online version in colour.)

5.2. Optimality in rectilinear locomotion

In rectilinear locomotion, snakes generate travelling waves prescribed by three kinematic variables, period τ, amplitude A and wavelength λ. We hypothesize rectilinear locomotion is optimal with respect to these variables. Consequently, we expect changes in these variables to result in lower body speed. In this section, we test this hypothesis using our model.

Figure 10a–c shows changes in body speed owing to variation of one kinematic variable, while keeping the other two variables and the friction coefficients fixed at their observed values for the Dumeril's boa. We find wave period and amplitude most influence body speed, whereas wavelength has little effect. We discuss these variables each in turn.

As shown in figure 10a, snake speed peaks at period $\tau = 1$ s. The period of snake locomotion from our experiments ($\tau = 2.1$ s) is close to the optimal period of wave propagation ($\tau = 1$ s) as shown in figure 10a, suggesting that snakes indeed choose the optimal period for maximizing speed. Deviations from the optimal period of 1 s result in slower speeds. Larger periods corresponding to slower wave propagation, or fewer steps per second, result in slower body speed. Less intuitively, smaller periods also reduce speed, a phenomenon we may rationalize using Froude number.

To compare inertia to friction in rectilinear locomotion, we redefine the Froude number as

$$Fr^* = A/(\mu_b \tau^2 g). \tag{5.1}$$

In this formulation, we replace body length L in equation (3.3) with amplitude A, which, for rectilinear locomotion, is a more accurate measure of local speed relative to ground. The friction coefficient μ_b is used to account for friction force. If period of motion is smaller than 0.18 s, then Fr^* will be larger than unity and, thus the inertial force will be greater than backward friction force. This inertia causes the
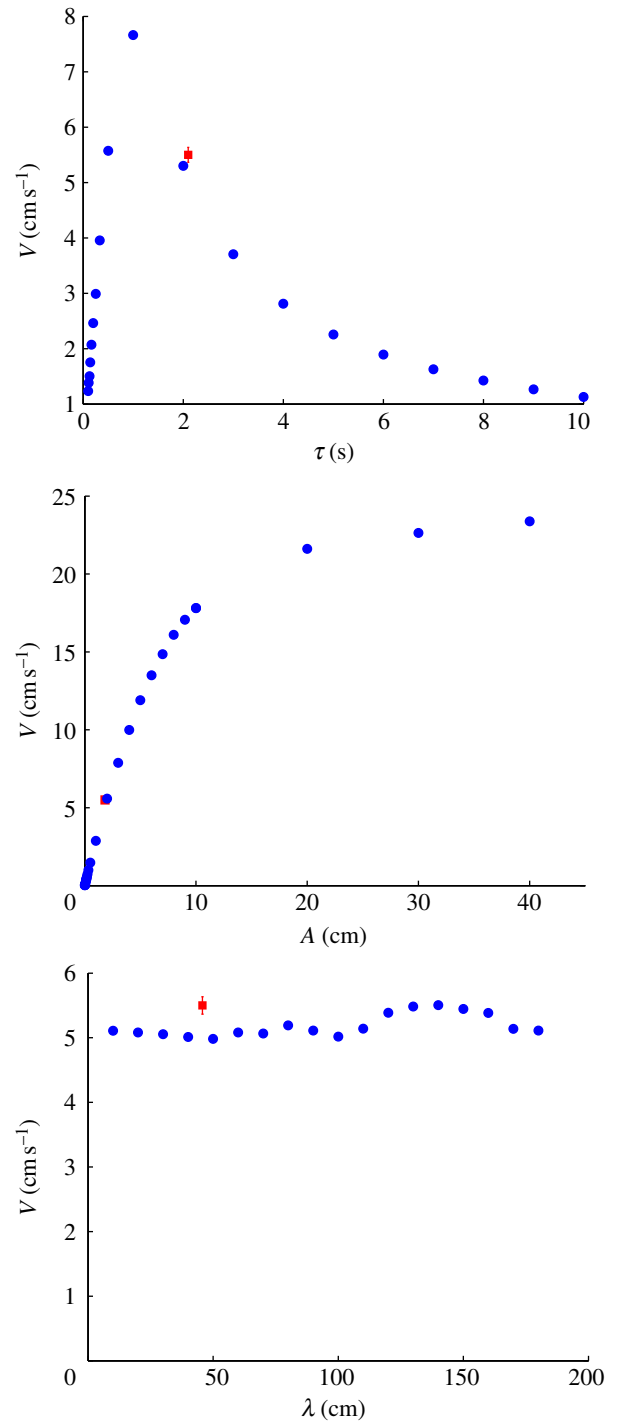

Figure 10. The relation between predicted body speed and changes in body kinematics. Variation in body speed as a function of (a) the period of wave propagation τ, (b) wave amplitude A and (c) wavelength λ as predicted by our mathematical model. Square data point shows experimental measurements for Dumeril's boa. Filled circles denote model. (Online version in colour.)

snake to slip backwards during rectilinear locomotion and slow down accordingly. An optimal wave period can be rationalized thus: snakes should keep their wave periods sufficiently high to remain in the low-Froude number regime, but not so high that they begin to decrease their speed.

Figure 10b shows the snake's choice of wave amplitude is suboptimal. In fact, increasing amplitude will increase body speed in the same way that taking longer steps increases the speed of walking. The maximum amplitude that can be taken before slipping occurs can also be rationalized using the Froude number: a wave amplitude larger than 2.6 m will make the inertial force greater than the friction force

and the snake will begin to slip. As a result, we expect a reduction in speed for amplitudes larger than 2.6 m. We do not observe such large amplitudes in nature because of the limiting strain in snake muscle.

Figure 10c shows wavelength does not affect body speed, at least on the homogeneous substrates we have studied. Wavelength prescribes the number of waves along the body at a given instant. In our simulation, we increase the number of waves from one to 200. We do not observe an optimum, because the number of waves does not affect the Froude number. As long as the Froude number is small, friction force is larger than inertial force, and the body continues to maintain its grip with the ground. Consequently, peak body speed is set by the wave amplitude and period; additional waves do not move the body faster.

The trends in figure 10 are qualitatively accurate for other snakes. We conducted the same optimality analysis for other species of snakes used in our experiments and we observed similar trends for all of them. Specifically, both red-tailed boas and Gaboon vipers have wave periods that are larger than the optimum values such that snakes are in the non-slipping regime. Moreover, their wave amplitudes are suboptimal and wavelengths do not impact body speed.

5.3. Benefits of lifting on surfaces of various roughness
Figure 11 shows the predicted relation between body speed and backwards friction coefficient. We present two trends, the body speed with body lifting (blue open points) and without lifting (red closed points). For the latter, we use our measured forward friction coefficients, which is 0.017 ± 0.002 for the Dumeril's boa. The friction coefficient and body speed measured for the Dumeril's boa is denoted by the black square. For this friction coefficient, lifting increases body speed by 31 per cent, indicating the importance of lifting behaviour, at least on the surfaces tested in our experiments. On other surfaces, lifting remains beneficial for forward movement. We investigate numerically the effects of lifting on speed for a range of values in backward friction coefficient.

At low values of backwards friction coefficient, locomotion is poor. If friction is zero ($\mu_b = 0$), then the lifted snake remains stationary during rectilinear locomotion. Such inability to move has also been seen in previous work on other gaits. Slithering on a featureless surface yields no net motion [4]. Correspondingly, the non-lifted snake remains stationary if the backwards friction coefficient is equal to the measured value of the forward friction coefficient, 0.017.

At low friction coefficients, lifted and non-lifted snakes differ in the speed as shown on the left-hand side of figure 11. In this regime, the combined effects of Froude number and friction anisotropy each affect locomotion. For non-lifted snakes, as friction coefficient μ_b decreases, Froude number increases and frictional anisotropy decreases. Both these effects cause slipping and so decrease body speed. By contrast, the lifted snake has infinite friction anisotropy for any non-zero backwards friction coefficient. Thus, it can undergo larger Froude numbers and thus larger inertial forces without a decrease in body speed. Thus, lifted snakes move more robustly than non-lifted snakes.

At intermediate friction coefficients, snakes increase in speed with increasing friction coefficient. Speed asymptotes at 5.5 cm s^{-1}. This asymptotic behaviour begins at a friction coefficient of 0.01 for lifted snakes and 0.1 for non-lifting
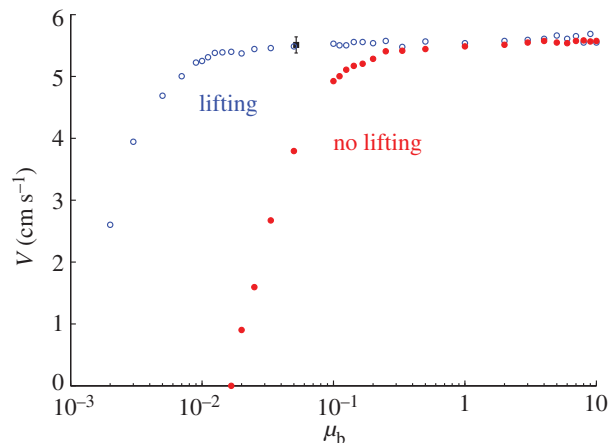

Figure 11. The relation between predicted body speed V and backwards friction coefficient μ_b. Speed of a snake lifting its body is compared with one without body lifting. The square data point shows experimental measurements for Dumeril's boa. Open circles denote model with lifting; filled circles denote model without lifting. (Online version in colour.)

snakes. Thus, lifted snakes have a larger range of surfaces they can climb upon while still maintaining their high speed.

At the highest friction coefficients ($\mu_b \geq 0.5$), lifting no longer improves body speed. In this regime, the Froude number Fr^* is smaller than 0.0008, and so the inertial force is infinitesimal, minimizing backwards body sliding during locomotion. Given that both simulations are prescribed by the same body kinematics, they converge to the same speed of 5.5 cm s^{-1}. Thus, on the roughest surfaces, which provide high friction coefficients, lifting does not necessarily increase body speed.

5.4. Energetics
Previously, we investigated how kinematics and friction coefficients affect body speed. A lumbering gait like rectilinear locomotion should have a low rate of working, or NCT. We hypothesize rectilinear locomotion has a smaller NCT than other gaits, because it is the slowest, and less energy is expended on inertia and lateral motion of body. We define a physical rate of work, or the partial cost of transport (PCT), which is a fraction of the NCT previously measured in snake metabolic experiments. We here use our model to estimate the scaling of PCT with body size.

The PCT of a snake performing rectilinear locomotion is the combination of work owing to gravity W_{gravity}, dissipation associated with body lifting D_{lifting} and inertia D_{inertia}. These terms are divided by snake mass m and the distance travelled in one period ΔL. Accordingly, this summation may be written

$$\text{PCT} = \frac{W_{\text{gravity}} + D_{\text{lifting}} + D_{\text{inertia}}}{m\Delta L}. \qquad (5.2)$$

The gravitational work performed by a segment of mass m_i is $m_i g z_i$, where z_i is the vertical displacement. Because $\sum_{i=1}^{n} m_i z_i = m z_c$, where $z_c = \sin\theta\Delta L$ is the vertical displacement of centre of mass, the work of gravity may be simplified as $mg\sin\theta\Delta L$, where m is the mass of the snake.

A snake lifts its segments to move them forward. We assume the energy used to lift a segment is not regained by the snake as useful work. Because all segments of the snake
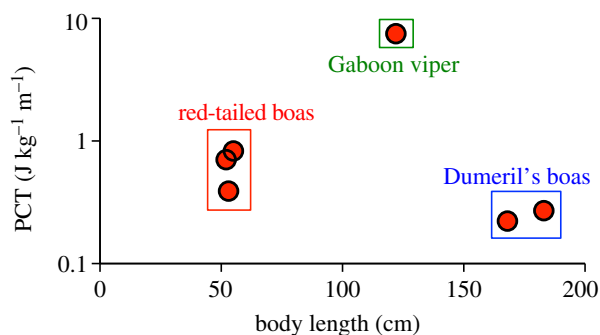
Figure 12. Calculated rate of working, or partial cost of transport (PCT) for three red-tailed boas, two Dumeril's boas and a Gaboon viper. (Online version in colour.)

are lifted once during a period, from the view of energetics, we can consider the entire body mg lifting simultaneously. The energy dissipation owing to a snake lifting its body is $mg\cos\theta\Delta h$, where Δh is the highest elevation of a segment.

The inertial losses associated with changing the snake's speed are given by $D_{inertia}$. Considering the change in the speed of each segment, $D_{inertia}$ may be written as $\sum_{i=1}^{n} m_i|\ddot{x}_i\Delta x_i|$, where m_i is the mass of ith segment, $\ddot{x}$ is the second-time derivative of $x(t,s)$ presented in equation (4.2) and Δx_i is the displacement of ith segment. As a result, equation (5.1) may be written as

$$PCT = g\sin\theta + \frac{g\cos\theta\Delta h}{\Delta L} + \frac{\sum_{i=1}^{n} m_i|\ddot{x}_i\Delta x_i|}{m\Delta L}. \quad (5.3)$$

Figure 12 illustrates PCT for three red-tailed boas, a Gaboon viper and two Dumeril's boas. The PCT for these snakes ranges between 0.22 and 7.5 J kg^{-1} m^{-1}. We do not account for the effect of snake metabolism in our calculation. Notwithstanding, our PCT estimates are up to an order of magnitude less than the NCT measures found for other snake gaits, consistent with the notion that rectilinear is indeed the most efficient gait.

By examining the relative magnitudes of the energies expended in the PCT, we can gain insights into the dominant energetics. Work done to lift the snakes, $D_{lifting}$, is dominant for red-tailed boas ($92 \pm 5\%$ of PCT). Conversely, work done against body inertia $D_{inertia}$ is dominant for both Gaboon viper (97% of PCT) and Dumeril's boas ($90 \pm 1\%$ of PCT). Why does the red-tailed boa spend more energy on lifting than the other two snakes? As shown in equation (5.2), the lifting energy scales as the dimensionless $\Delta h/\Delta L$. The red-tailed boa lifts the highest of the snakes. Consequently, it has values of $\Delta h/\Delta L$ which are two to 15 times that for the other snakes, and so a correspondingly high lifting energy.

6. Discussion

6.1. Unique wave frequency scaling

Our study of rectilinear locomotion yields new insights into the fundamental differences between legged and legless locomotion. In both types of locomotion, we can characterize a frequency of bodily contacts with the ground. Legged animals exhibit decreasing frequencies with increasing body size. For example, elephants have lower leg frequencies than much
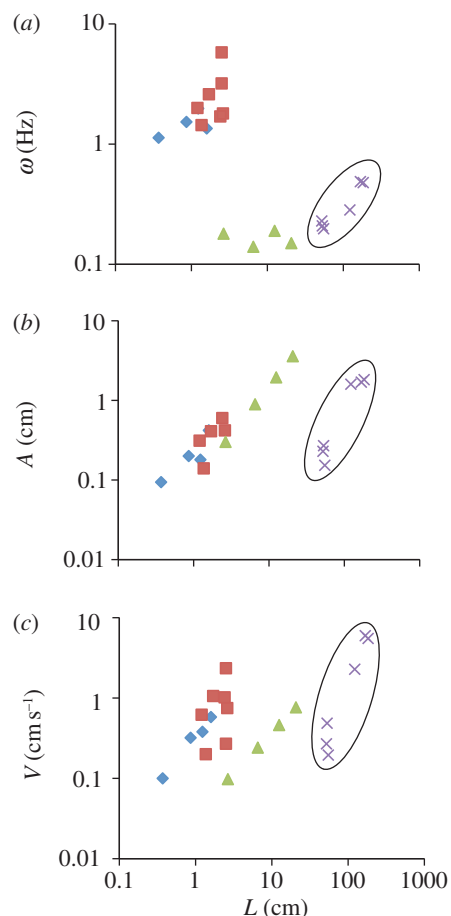

Figure 13. The relation between body length L and (a) wave frequency ω, (b) wave amplitude A and (c) body speed V for several rectilinear movers, including maggots (diamonds) [23], caterpillars (squares) [24–27], earthworms (triangles) [28,29] and snakes (purple multiplication symbols). (Online version in colour.)

smaller animals such as mice. The reason for this trend is well known [12,19]: larger animals are more massive, and given the same specific muscular power, move more slowly and so have lower frequencies. This trend also extends to certain gaits in limbless locomotion. In concertina and lateral undulation, larger snakes also have lower frequencies [20–22].

Surprisingly, we find the opposite trend in rectilinear locomotion: larger animals tend to have higher frequencies, increasing by more than a factor of two, from 0.2 to 0.5 Hz, as snake length increases from 52 to 183 cm. This trend is clearly limiting for large snakes. Is this trend universal across other animals that use unidirectional motion? To answer this question, we compare rectilinear kinematics with those previously measured for other animals, including maggots [23], caterpillars [24–27] and earthworms [28,29]. Figure 13a–c shows the results of this comparison.

Figure 13a shows the relation between frequency and body length. We find snakes are the only rectilinear movers to have increasing frequency with increasing body size ($p < 0.0001$). Caterpillar, maggots and earthworms maintain nearly constant frequency with size ($p = 0.35, 0.56$ and 0.78, respectively). In particular, the earthworm maintains a relatively constant frequency over a factor of 10 increase in body length (only 17% decrease in frequency). This is very different from the trend for snakes. Nevertheless, both earthworms and snakes appear to fit well along the same power law scaling ($\omega = 0.12L^{0.143}$, $r^2 = 0.84$). The accuracy of this

trend line suggesting that their motion is indeed similar, despite quite different methods for generating force (hydrostatic pressure versus muscles).

Earthworms and snakes also tend to fit in the same category if their frequency range is compared with other animals. In figure 13a, there exist two discrete regimes in frequency. Large animals such as snakes and earthworms ($\omega = 0.14 - 0.5$ Hz) have 10 times lower frequencies than small animals such as maggots and caterpillars ($\omega = 1.1 - 5$ Hz).

Figure 13b,c shows trends for amplitude and speed among maggots, caterpillars, earthworms and snakes. Larger animals, with the exception of caterpillars, have greater amplitudes and faster speeds. This trend is typical in legged locomotion as well [12]. In terms of amplitude, maggots, caterpillars and worms again fall on a single trend line ($A = 0.168L$, $r^2 = 0.98$): their amplitudes are 17 per cent of their body length. In comparison, snakes performing rectilinear locomotion have much smaller amplitudes (1% of body length). As we saw earlier in §5.2, snakes would benefit from increasing their amplitude in rectilinear locomotion. This inability likely arises from the contractile–extensile limits of their muscles, which can be bypassed by worms because of their reliance on hydrostatic pressure.

6.2. Improving rectilinear locomotion

Rectilinear locomotion is quite a slow gait, achieving only $0.2 - 6$ cm s^{-1} for snakes of length 50–180 cm. It is best used for creeping up on prey and other activities requiring stealth. Are there any behaviours that can increase the speed or efficiency of the gait?

We measured the range of inclination angles that snakes can perform rectilinear locomotion. We observed the maximum angles snakes can climb on Styrofoam are all quite low: they are 15°, 6° and 3°, respectively, for red-tailed boas, Gaboon vipers and Dumeril's boas. At higher inclination angles, snakes will attempt to climb using rectilinear motion, but inevitably slide down. Thus, rectilinear locomotion alone cannot be used to climb sheer vertical surfaces. Tree-climbing snakes ascending trees by using different parts of their body performing concertina or rectilinear locomotion, exploiting interstices and other features of the tree opportunistically. Thus, rectilinear locomotion should be used in combination with other snake gaits to be effective.

7. Conclusion

In this study, we report on the rectilinear locomotion of snakes. We characterize the kinematics of a snake's travelling wave using measurements of wave speed, amplitude and frequency. We discover scaling trends in rectilinear locomotion which contrast strikingly to those of other snake gaits and animal locomotion in general. In particular, wave frequency increases with increasing body size for snakes performing rectilinear motion. Such a trend is anomalous for legged animals [12,19] and other rectilinear movers such as maggots, earthworms and caterpillars.

We report a theoretical crawler model to investigate how snake behaviours, such as lifting and kinematics, influence performance in terms of body speed and efficiency. Inputs to our model are the kinematics of the travelling wave and the frictional properties of snakes. The model output is the speed of a snake's centre of mass, which compares favourably with experiments (73–97% accuracy). During our experiments, we observe snakes lift parts of their bodies during rectilinear locomotion, and we hypothesize they do so to reduce frictional dissipation. Our model shows that localized body lifting increases the speed of a Dumeril's boa rectilinear locomotion by 31 per cent. This result is similar to previous simulations on slithering locomotion, in which lifting increases body speed by 35 per cent [4].

We identify which wave parameters are optimal in rectilinear propulsion. We show this result by using our model to calculate snake speed over a range of kinematic variables. The wave frequency chosen by a Dumeril's boa is close to optimum: higher frequencies cause slipping and lower frequencies decrease thrust and slow the snake. The snake's amplitude, however, is suboptimal and is likely limited by anatomical constraints. Lastly, we find wavelength does not influence body speed on uniform surfaces. Instead, it may help with robustness of the gait's interactions with ground contacts. Having a smaller wavelength is similar to walking with a greater number of feet, which may help in tackling surfaces with frequent imperfections.

References

1. Wright C, Johnson A, Peck A, McCord Z, Naaktgeboren A, Gianfortoni P, Gonzalez-Rivero M, Hatton R, Choset H. 2007 Design of a modular snake robot. In IEEE/RSJ Int. Conf. on Intelligent Robots and Systems, San Diego, CA, 29 October to 2 November 2007, pp. 2609–2614. New York, NY: IEEE.

2. Erkmen I, Erkmen A, Matsuno F, Chatterjee R, Kamegawa T. 2002 Snake robots to the rescue! IEEE Robot. Autom. Mag. 9, 17–25. (doi:10.1109/MRA.2002.1035210)

3. Webster R, Okamura A, Cowan N. 2006 Toward active cannulas: miniature snake-like surgical robots. In IEEE/RSJ Int. Conf. on Intelligent Robots and Systems, Beijing, China, 9–15 October, pp. 2857–2863. New York, NY: IEEE.

4. Hu D, Nirody J, Scott T, Shelley M. 2009 The mechanics of slithering locomotion. Proc. Natl Acad. Sci. USA 106, 10 081–10 085. (doi:10.1073/pnas.0812533106)

5. Secor SM, Jayne BC, Bennett AC. 1992 Locomotor performance and energetic cost of sidewinding by the snake Crotalus cerastes. J. Exp. Biol. 163, 1–14. (doi:10.1016/0022-0981(92) 90143-X)

6. Marvi H, Hu D. 2012 Friction enhancement in concertina locomotion of snakes. J. R. Soc. Interface 9, 3067–3080. (doi:10.1098/rsif.2012.0132)

7. Home E. 1812 Observations intended to show that the progressive motion of snakes is partly performed by means of the ribs. Phil. Trans. R. Soc. Lond. 102, 163–168. (doi:10.1098/rstl. 1812.0011)

8. Mosauer W. 1932 On the locomotion of snakes. Science 76, 583–585. (doi:10.1126/science.76. 1982.583)

9. Bogert C. 1947 Rectilinear locomotion in snakes. Copeia 1947, 253–254. (doi:10.2307/1438921)

10. Lissman HW. 1950 Rectilinear locomotion in a snake (Boa occidentalis). J. Exp. Biol. 26, 368–379.

11. Walton M, Jayne BC, Bennett AF. 1990 The energetic cost of limbless locomotion. Science 249, 524–527. (doi:10.1126/science.249.4968.524)

12. Alexander RM. 2003 Principles of animal locomotion. Princeton, NJ: Princeton University Press.

13. Keller J, Falkovitz M. 1983 Crawling of worms. J. Theor. Biol. 104, 417–442. (doi:10.1016/ 0022-5193(83)90115-7)

14. Gray S. 1968 *Animal locomotion*. London, UK: Weidenfeld & Nicolson.

15. Zimmermann K, Zeidis I. 2007 Worm-like locomotion as a problem of nonlinear dynamics. *J. Theor. Appl. Mech. (Warsaw)* **45**, 179.

16. Mehrtens J. 1987 *Living snakes of the world in color*. New York, NY: Sterling.

17. Mosauer W. 1935 How fast can snakes travel? *Copeia* **1**, 6–9. (doi:10.2307/1436627)

18. Dormand J, Prince P. 1980 A family of embedded Runge–Kutta formulae. *J. Comput. Appl. Math.* **6**, 19–26. (doi:10.1016/0771-050X(80)90013-3)

19. Schmidt-Nielsen K. 1984 *Scaling, why is animal size so important*? Cambridge, UK: Cambridge University Press.

20. Gans C, Gasc J. 1990 Tests on the locomotion of the elongate and limbless reptile *Ophisaurus apodus* (Sauna: Anguidae). *J. Zool.* **220**, 517–536. (doi:10.1111/j.1469-7998.1990.tb04731.x)

21. Jayne B, Davis J. 1991 Kinematics and performance capacity for the concertina locomotion of a snake (*Coluber constrictor*). *J. Exp. Biol.* **156**, 539.

22. Renous S, Hofling E, Gasc JP. 1995 Analysis of the locomotion pattern of two microteiid lizards with reduced limbs, *Calyptommatus leiolepis* and *Nothobachia ablephara* (Gymnophthalmidae). *Zoology* **99**, 21–38.

23. Berrigan D, Pepin D. 1995 How maggots move: allometry and kinematics of crawling in larval diptera. *J. Insect Physiol.* **41**, 329–337. (doi:10.1016/0022-1910(94)00113-U)

24. Brackenbury J. 1999 Fast locomotion in caterpillars. *J. Insect Physiol.* **45**, 525–533. (doi:10.1016/S0022-1910(98)00157-7)

25. Brackenbury J. 2000 Locomotory modes in the larva and pupa of chironomus plumosus (Diptera, Chironomidae). *J. Insect Physiol.* **46**, 1517–1527. (doi:10.1016/S0022-1910(00)00079-2)

26. Joos B. 1992 Adaptations for locomotion at low body temperatures in eastern tent caterpillars, *Malacosoma americanum*. *Physiol. Zool.* **65**, 1148–1161.

27. Casey T. 1991 Energetics of caterpillar locomotion: biomechanical constraints of a hydraulic skeleton. *Science* **252**, 112–114. (doi:10.1126/science.252.5002.112)

28. Quillin K. 1999 Kinematic scaling of locomotion by hydrostatic animals: ontogeny of peristaltic crawling by the earthworm lumbricus terrestris. *J. Exp. Biol.* **202**, 661–674.

29. Quillin K. 2000 Ontogenetic scaling of burrowing forces in the earthworm lumbricus terrestris. *J. Exp. Biol.* **203**, 2757–2770.